University of Birmingham
Research at Birmingham

# Ideal performance of a self-cooling greenhouse

Davies, Philip A.; Zaragoza, Guillermo

*DOI:*
10.1016/j.applthermaleng.2018.12.056

*License:*
Creative Commons: Attribution-NonCommercial-NoDerivs (CC BY-NC-ND)

*Document Version*
Peer reviewed version

*Citation for published version (Harvard):*
Davies, PA & Zaragoza, G 2019, 'Ideal performance of a self-cooling greenhouse', *Applied Thermal Engineering*, vol. 149, pp. 502-511. https://doi.org/10.1016/j.applthermaleng.2018.12.056

Link to publication on Research at Birmingham portal

**Publisher Rights Statement:**
Checked for eligibility: 19/12/2018

**General rights**
Unless a licence is specified above, all rights (including copyright and moral rights) in this document are retained by the authors and/or the copyright holders. The express permission of the copyright holder must be obtained for any use of this material other than for purposes permitted by law.

•Users may freely distribute the URL that is used to identify this publication.
•Users may download and/or print one copy of the publication from the University of Birmingham research portal for the purpose of private study or non-commercial research.
•User may use extracts from the document in line with the concept of 'fair dealing' under the Copyright, Designs and Patents Act 1988 (?)
•Users may not further distribute the material nor use it for the purposes of commercial gain.

Where a licence is displayed above, please note the terms and conditions of the licence govern your use of this document.

When citing, please reference the published version.

**Take down policy**
While the University of Birmingham exercises care and attention in making items available there are rare occasions when an item has been uploaded in error or has been deemed to be commercially or otherwise sensitive.

If you believe that this is the case for this document, please contact UBIRA@lists.bham.ac.uk providing details and we will remove access to the work immediately and investigate.

Download date: 27. Apr. 2024

# Ideal performance of a self-cooling greenhouse

Philip A. Davies[1]* and Guillermo Zaragoza[2]

1. Sustainable Environment Research Group, School of Engineering and Applied Science, Aston University, Birmingham, B4 7ET, UK
2. CIEMAT, Plataforma Solar de Almería, Ctra. de Senés s/n, 04200 Tabernas, Almería, Spain

* p.a.davies@bham.ac.uk

**Abstract:** The self-cooling greenhouse is a concept to enable crop cultivation in adversely hot climates. It sacrifices a fraction $\gamma$ of the incident solar energy to drive a refrigeration system, thus lowering the internal temperature below ambient. Heat is actively rejected to a stream of coolant such as air or water. To maintain availability of sunlight for photosynthesis, $\gamma$ should be as small as possible. Nonetheless, the laws of thermodynamics dictate a minimum value of $\gamma$. Using the approach of endoreversible thermodynamics and the theory of selective blackbody absorbers, we determine ideal minimum values achievable for cases of both thermal and photovoltaic solar collection with and without solar concentration. To achieve an internal temperature 10°C below that of the incoming coolant, a minimum $\gamma$=0.056 is needed using multicolour absorption at maximum concentration $C$=46300 – representing an absolute minimum for either type of solar collection. Without concentration ($C$=1) a selective thermal collector permits minimum $\gamma$ =0.089 and a single-junction PV solar collector permits minimum $\gamma$ =0.15. We discuss briefly implications for development of a real self-cooling greenhouse to approximate the performance of these ideal cases.

**Keywords:** Solar refrigeration; greenhouse cooling; solar thermal; solar PV; thermodynamic limit; endoreversible.

## Nomenclature

| Symbol | Unit | Description |
|---|---|---|
| $A$ | $m^2$ | Area of PV cell or thermal receiver |
| $c$ | $m\ s^{-1}$ | Speed of light in a vacuum |
| $c_p$ | $J\ kg^{-1}\ K^{-1}$ | Specific heat capacity of coolant at constant pressure |
| $C$ | | Concentration ratio |
| $COP$ | | Coefficient of performance |
| $E$ | eV | Energy level of photon |
| $E_g$ | eV | Bandgap |
| $f$ | | Solar dilution factor |
| $h$ | J s | Planck's constant |
| $k$ | $J\ K^{-1}$ | Boltzmann constant |
| $m$ | $kg\ s^{-1}$ | Mass flow of coolant |
| $N$ | $s^{-1}$ | Net rate of photon absorption by PV cell |
| $q$ | $eV\ V^{-1}$ | Elementary charge ($q$=1) |
| $Q_h$ | W | Heat flow from solar collector to refrigerator |
| $\delta Q_i$ | W | Heat flow from $i$'th solar collector |
| $Q_{int}$ | W | Heat flow from interior of greenhouse to refrigerator |
| $Q_{sun}$ | W | Radiative heat flow from sun to greenhouse |
| $T_{c1}$ | K | Temperature of coolant at inlet |
| $T_{c2}$ | K | Temperature of coolant at inlet |
| $T_{cell}$ | K | Temperature of PV cell |
| $T_h$ | K | Temperature of solar collector |
| $T_i$ | K | Temperature of the $i$'th collector |
| $T_{int}$ | K | Temperature of interior of greenhouse |
| $T_{sky}$ | K | Effective temperature of sky |
| $T_{sun}$ | K | Effective temperature of Sun |
| $\bar{T}$ | K | Log mean temperature |
| $V$ | V | Bias voltage of PV cell |
| $W$ | W | Work done by the solar cell |
| $\gamma$ | | Fraction of greenhouse shaded by solar collector |
| $\eta$ | | Efficiency of solar collection or conversion |
| $\lambda$ | | Fraction of solar radiation thermalized by PV cell |

Note since $E$ is measured in eV and $Q_{sun}$ in watts, a conversion factor of $1.602 \times 10^{-19}$ J/eV is applied after use of $E$ and $E_g$ in Planck's law in the numerical calculations.

## Abbreviations

COP Coefficient of performance
PV Photovoltaic

## 1. Introduction

Increasing ambient temperatures and growing populations require new methods for cultivation of crops under adverse conditions. Global temperatures from 2013-2017 showed the highest five-year average on record [1]. In many instances, regions having some of the hottest climates are also experiencing exceptionally fast population growth; for example, Pakistan, Egypt and Somalia are expected to see population increase by 24%, 27% and 46% respectively between 2017 and 2030 compared to the global average of only 14% over the same period [2]. The vulnerability of such populous and agriculturally-dependent countries to changing climate is a serious cause for concern [1].

Protected cultivation of crops within greenhouses is a way to maintain and increase crop yields despite climate variability. Unlike in open-field cultivation, conditions can be kept at desired levels by heating and cooling systems. In hot climates, cooling is needed, for which a number of technologies have been proposed or are already in use. These include shading, ventilation, earth-to-air heat exchangers, fogging, and evaporative cooling with pad-and-fan systems [3, 4].

Evaporative cooling is currently the preferred technology for greenhouse cooling in hot climates; but its performance is limited, especially under humid conditions, as it cannot cool below the wet-bulb temperature [5]. Lower temperatures are achievable using vapour compression refrigerators [6, 7]. Nonetheless, such refrigerators use excessive energy when scaled up to the multi-hectare installations common in commercial crop production. Use of conventional energy resources for greenhouse cooling by vapour compression refrigerators, or by other active systems, would be unlikely to provide a sustainable solution for crop production in coming years. Since, however, solar energy is naturally abundant at locations and times of year where cooling is most needed, it makes sense to investigate cooling of greenhouses powered by the sun.

The challenge in any solar-powered cooling is the large solar collection area potentially required, which could increase markedly the footprint of a greenhouse. For example, Puglisi, et al. [8] developed a solar-powered absorption refrigeration to cool a greenhouse in Italy, for which they required an area of solar collector comparable in size to the greenhouse itself. Lychnos and Davies [9] investigated the feasibility of greenhouse cooling by means of a solar-powered liquid desiccant cycle with an open collector-regenerator. Depending on location and ambient conditions, the collector-regenerator was predicted to occupy 0.5 to 4.5 times the greenhouse plan area.

In this study, we propose that it would be advantageous to devise a greenhouse cooling system whereby the solar energy collection is compactly integrated into the greenhouse, without occupying any external footprint. If realised, such a concept could be termed a *self-cooling greenhouse*. The challenge for the design of the self-cooling greenhouse is whether it can be made efficient enough to achieve low temperatures without robbing the plants of incoming solar energy such as to slow down growth and decrease crop yield significantly.

With the motivation of minimising the total footprint of energy production and agriculture, numerous researchers modelled and developed the integration of solar collectors (especially photovoltaic, PV, type) with greenhouse structures and cladding [10-15]. As in the current study, some have investigated the degree of shading created by the solar collectors and how this affects overall feasibility. The studies are not limited to small prototypes but include commercial-scale installations. Pérez-Alonso et al. [13], for example, constructed and monitored a 1024 $m^2$ pilot greenhouse incorporating amorphous silicon solar cells externally fixed to the greenhouse cover, shading 9.72% of the roof area in a checkerboard pattern. Hassanien et al.[15] evaluated building-integrated crystalline PV cells comparing them against conventional greenhouse cladding in greenhouses of 26 $m^2$ footprint. With 20% shading, they observed no significant loss of yield in a tomato crop. Castellano et al.[16] reported a 500 $m^2$ greenhouse installation in which the roof was entirely obscured by crystalline solar PV panels, with light entering by the side walls only. They studied the photon flux both numerically and experimentally, though did not report on the crop yield. Micro-spherical crystalline silicon PV-cells have also been used, sandwiched between glass panes constituting the greenhouse cladding.[14] Similar micro-spherical cells have been used in venetian blind arrangements, in a prototype greenhouse of 24 $m^2$ floor area [17, 18]. Instead of silicon, Emmott, et al. [19] proposed using organic PV, highlighting its potential for selective light absorption and low cost. Allardyce, et al. [20] highlighted the potential of dye-sensitized cells for selective absorption and increased biomass yield. Dupraz, et al. [21] calculated that the integration of photovoltaics with greenhouses can make better overall use of land, compared to when agricultural and energy harvesting are kept separate. Nonetheless, the above researchers considered the integration of solar PV for electricity production mainly, and not specifically for active greenhouse cooling.

In a self-cooling greenhouse, the amount of sunlight sacrificed for refrigeration should be minimized – because the light is needed for photosynthesis primarily. According to Marcelis, et al. [22], reduction in light intensity by 1% generally results in a reduction in yield of between 0.7 and 1% for greenhouse crops. The exact relation depends on a number of factors e.g. the species, $CO_2$ concentration, spectral composition of the light, temperature, and nutrient levels [23]. At higher light levels, the sensitivity of yield with respect to intensity is generally decreased, because of the limiting effect of other factors such as $CO_2$ concentration [23, 24]. Aggregated data showed that a 33% reduction in light intensity (starting from 6 $kWh/m^2$.day) resulted in a 20% average reduction in the yield of cucumber [22]. This suggests that the sacrifice of light should be <30% approximately for good crop yield to be maintained.

A self-cooling greenhouse will need to reject heat to the surroundings. For this purpose, a cooling fluid (coolant) will be required as a heat sink. Most likely this fluid will be water or air. Water is an excellent coolant due its high heat capacity and thermal conductivity. Thus in coastal locations, seawater appears to be an attractive coolant, as it is abundantly available. Elsewhere, water from aquifers or rivers might be used. A preliminary calculation shows that the flow of water (or other fluid) tends to be large. For example, a 1 hectare greenhouse receiving 1 $kW/m^2$ of solar irradiance generates a heat load of approximately 10 MW, enough to heat a stream of water flowing at 0.25 $m^3/s$ by about 10°C. To minimize capital and operating costs of associated pipeline construction and pumping, it is therefore desirable that this flow be kept to a minimum for a given target temperature inside the greenhouse.

Using generalised assumptions about the cooling fluid and other aspects, this paper considers the feasibility of a self-cooling greenhouse from a fundamental thermodynamic perspective. To the authors' knowledge, such a fundamental study has not been undertaken. To address the gap, this paper aims to establish the ideal limits to performance based on the laws of thermodynamics. Typical design objectives for a self-cooling greenhouse would be to:

i. Achieve a substantial temperature drop (say 15°C) inside the greenhouse relative to ambient
ii. Incur minimum sacrifice of light (say <30%) in driving the refrigeration process
iii. Require minimum flow of coolant to remove the heat.

These three objectives conflict; therefore it is important to quantify and understand the relations among them. This paper explores these relations by establishing ideal models of the self-cooling greenhouse, thus allowing the trade-offs among the design objectives to be investigated. The analysis sets out to be as general as possible, establishing limits according to general principles with minimal dependence on the technological designs and materials used. Such an idealised study is useful to provide a benchmark against which real systems or proposed design concepts can be evaluated.

The concept of an idealised performance based on thermodynamic principles is already well established in solar energy research. We could cite, for example, the works by Shockley and Queisser [25] and by Trivich and Flinn [26] on the limiting performance of PV cells, and the many subsequent works building on those (e.g. [27-31]). We could also cite comparable seminal works in the area of solar thermal energy conversion such as those of Castañs [32] and De Vos [33]. Although those works did not set out many technological details of specific devices, they gave general results that were very useful to guide practical developments of solar energy collection devices subsequently. Similarly it is hoped that the current study will guide development of future self-cooling greenhouses.

First we explain the concept and assumptions used in the analyses, then present the mathematical analyses themselves for different cases covering both thermal and PV collection. This is followed by a general analysis for the ultimate thermodynamic performance of an ideal self-cooling greenhouse. Sensitivity analyses are included to assess the effect of varying the baseline assumptions. Finally, we discuss briefly technologies and prospects for implementation of real systems intended to approximate the ideal limits in practice; and we propose topics for future study.

## 2. Concept and assumptions

As an idealized case, the self-cooling greenhouse is conceptualized as a box with a transparent and horizontal roof that transmits perfectly incident solar radiation, at the same time insulating against all convective and conductive heat transfer. The box includes a refrigeration system that rejects heat to a flowing stream of coolant (Fig. 1). The only loss in solar transmission is that corresponding to the fraction $\gamma$ of energy diverted to the solar collector used to drive the refrigeration system. The remaining fraction ($1-\gamma$) is assumed to be absorbed entirely by the crops and soil inside the greenhouse – which behave as black body absorbers. The solar collector may be contained inside the greenhouse, or its surface may be integrated in the roof. It is assumed that the solar collector is completely opaque, such that $\gamma$ equals the area fraction occupied geometrically by the collector.

Like in many works aimed at determining the ideal performance of solar energy conversion processes (e.g. [32, 33]), the sunlight is modelled as blackbody radiation. This assumption is justified since self-cooling greenhouses would most likely be used in sunny climates where relatively clear-sky conditions are common. It is also assumed that the radiation falls perpendicularly on the greenhouse roof, because this type of greenhouse would typically be used at low latitudes (10-35°). Approximately overhead sunlight and clear sky conditions will tend to coincide with the times of day and year when the cooling system is most needed, and thus represent the appropriate assumptions. Moreover, more specific assumptions would limit the study to whatever particular solar radiation conditions were chosen, resulting in a loss of generality.

Solar and heat gain through the side walls of the greenhouse are assumed negligible. This assumption is justified by the fact that the greenhouse is intended for production of bulk quantities of crops to improve food security, and as such should cover extensive areas (e.g. several hectares) such that the sidewalls are very small in area compared to the roof. The assumption also has the advantage of making the results independent of the size, orientation and geometry of greenhouse.

An initial assumption is that the long-wave radiative heat transfer between the greenhouse and sky is negligible. To justify this assumption, we note that effective sky temperatures are typically 5-20°C below ambient [34, 35] and that a practical aim would be to cool the greenhouse by approximately similar amounts; therefore the interior temperature ($T_{int}$) is likely to be fairly close to the sky temperature, resulting in a long-wave heat flux that is much less than the solar radiation flux of order 1000 W/m$^2$. (This assumption will be further verified in the Discussion section). In contrast, radiative heat transfer from the solar collector to the sky is *not* neglected because, as will be seen, the collector may require to be operated at a temperature much higher than ambient (in the case of a thermal collector) or it may suffer inevitable radiative losses (in the case of a photovoltaic collector). Important constants and baseline values of the main parameters, as needed to initiate the analysis, are summarised in Table 1.

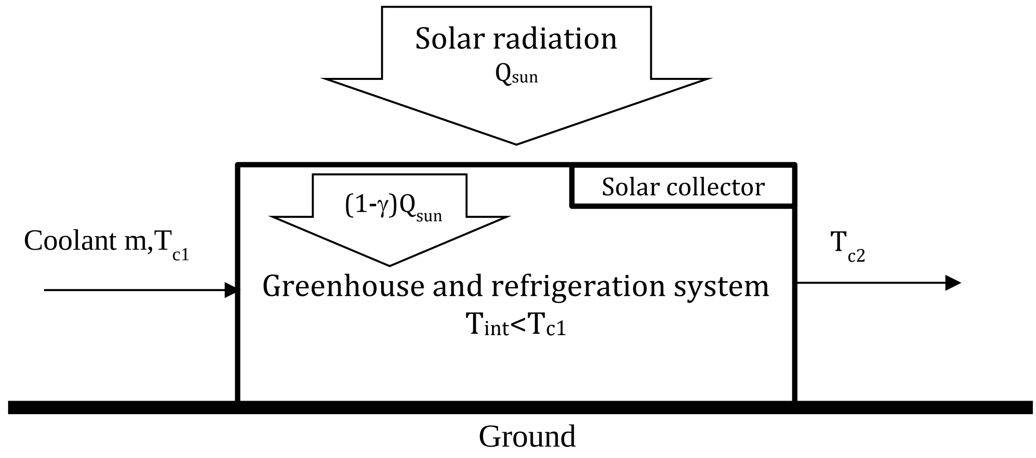


**Figure 1**: Idealized self-cooling greenhouse with transparent insulative roof, housing a solar energy collector that powers a refrigeration system. Heat is removed from the system by a coolant (e.g. seawater) with mass flow $m$, entering the box at temperature $T_{c1}$ and leaving at $T_{c2} > T_{c1}$. The greenhouse internal temperature $T_{int}$ must be maintained below $T_{c1}$. To drive the cooling system requires a fraction γ of the incoming solar radiation $Q_{sun}$ to be sacrificed to the solar collector. The goal is to minimise γ. The solar collector, shown here schematically as a single unit, could in practice be configured as several units distributed over the roof area of the greenhouse.

**Table 1**: Fixed and baseline parameters used in the analysis.

| Parameter | Unit | Value | Notes |
|---|---|---|---|
| Effective Sun temperature, $T_{sun}$ | K | 5762 | Approximating solar radiation as a blackbody [36, 37]. Different authors have used slightly different values e.g. Castañs [32] used 5770 K. |
| Solar dilution factor, $f$ | | $2.16 \times 10^{-5}$ | As used by De Vos [36], referring to the solar irradiance reaching the Earth as a fraction of that at the Sun's surface. Different sources used slightly different values as indeed the distance between the Sun and Earth varies due to ellipticity of orbit causing $f$ to vary. |
| Coolant inlet temperature, $T_{c1}$ | K | 303 | This value (30°C) is representative of a warm sea such as the Red Sea in July to September [38]. |
| Coolant outlet temperature, $T_{c2}$ | K | 313 | Cooling water in coastal power stations typically returns to the sea with a 8-10°C increase in temperature, so a 10°C increase is assumed here [39]. A range of 300-380 K is also considered. |
| Target interior temperature, $T_{int}$ | K | 293 | This value of 20°C represents benign conditions for cultivation of temperate or subtropical crops according to the species and cultivation regime [40]. A range of 280-310 K is also considered. |
| Sky temperature, $T_{sky}$ | K | 293 | Sky temperature is typically below ambient [34, 35] and taken here as approximately equal to $T_{int}$. Values of $T_{int}$ ±10°C are also considered in the sensitivity analysis. |

## 3. Approach

Because this is an idealized thermodynamic analysis, the natural starting point is to assume reversible processes that do not increase the entropy of the surroundings. However, collection of solar energy is not a reversible process, because a solar collector has to operate at a temperature below that of the sun to allow net heat transfer to occur. The term 'endoreversible' has been used to describe solar energy conversion in the sense that reversibility only applies *inside* the solar energy conversion process. Similarly the self-cooling greenhouse is considered to be an endoreversible machine [36, 41]. The internal processes of solar energy conversion and refrigeration are assumed reversible, without consideration being given for example to the sizing of components for heat transfer in the refrigeration cycle.

Many results have been presented for the idealized efficiency of solar energy converters of both thermal and photovoltaic (PV) types [27, 29, 30, 33, 36]. Typically, these studies present efficiency as a function of just two temperatures: (i) the sun temperature, and (ii) the planet or sink temperature which is typically assigned a nominal value of say 290 K or 300 K [27, 32]. This current study builds on these earlier works, by considering such idealized converters driving a perfect reversible heat pump to remove heat from a greenhouse. A new feature is the flow restriction in the coolant, which means that a single sink temperature for the system cannot be assumed. Both the input and output temperatures of the coolant are important, as well as the sun temperature, giving three main input temperatures to determine $\gamma$.

To make the analysis as general as possible, this study broadly follows the approach of De Vos [36], in that it sets out to rely on a justifiably minimum number of input parameters and assumptions about the physical processes used, thus providing results that are as general as possible. Nonetheless, separate analyses are needed for the cases of solar thermal and solar photovoltaic conversion processes because of the fundamental physical differences between these two types of process. After considering the separate cases, we will present a general analysis to represent ultimate ideal performance applying to both.

## 4. Case of solar thermal collector

For the case of the solar thermal collector, we include sub-cases with and without selective optical coating as used to reduce re-radiation of energy. For this case generally, we propose a thermally-driven refrigerator $R$ that receives a driving heat flow $Q_h$ [W] at temperature $T_h$ [K] from the solar collector and absorbs heat $Q_{int}$ [W] from the interior of the greenhouse at $T_{int}$ (Fig. 2). A thermally-driven refrigerator could consist of a heat engine coupled mechanically to a heat pump; or it could use concepts based on vapour absorption cooling or liquid desiccant cooling, or on some other concept. Since $R$ is assumed reversible, however, we can ignore its internal mechanisms and consider only the entropy flows at its boundary, which must sum to zero.

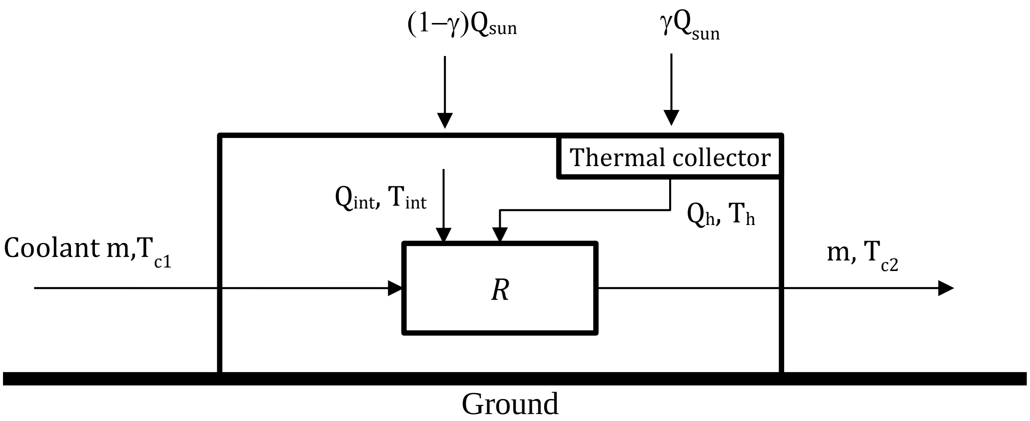


**Figure 2**: Case for the self-cooling greenhouse powered by a solar thermal collector delivering heat at rate $Q_h$ to a reversible refrigerator $R$.

Accordingly, the entropy balance gives:

$$\frac{Q_h}{T_h} + \frac{Q_{int}}{T_{int}} = mc_p \ln \frac{T_{c2}}{T_{c1}} \tag{1}$$

and the enthalpy balance gives:

$$Q_h + Q_{int} = mc_p(T_{c2} - T_{c1}) \tag{2}$$

where $m$ [kg/s] is the mass flow of the coolant and $c_p$ [kJ/kg K] is its specific heat capacity. The coolant has been assumed to be at constant pressure but, for nearly incompressible fluids like water, the equations remain valid even with moderate changes in pressure.

Defining the coefficient of performance of the thermally-driven refrigerator as $COP = Q_{int}/Q_h$, we combine (1) and (2) to get:

$$COP = \frac{1 - \bar{T}/T_h}{\bar{T}/T_{int} - 1} \tag{3}$$

where $\bar{T}$ is the logarithmic mean of $T_{c1}$ and $T_{c2}$,

$$\bar{T} = \frac{T_{c2} - T_{c1}}{\ln(T_{c2}/T_{c1})} \tag{4}$$

Now $Q_{int}$ is supplied by the solar radiation falling on the fraction (1-γ) of the greenhouse not shaded by the solar collector:

$$Q_{int} = (1 - \gamma)Q_{sun} \tag{5}$$

while $Q_h$ is equal to the radiation falling on the solar collector (occupying fraction $\gamma$ of the greenhouse roof area) multiplied by its efficiency $\eta$,

$$Q_h = \eta \alpha Q_{sun} \qquad (6).$$

Combining eqs (5) and (6) with the definition $COP = Q_{int}/Q_h$ and re-arranging gives an expression for the minimum fraction of shading needed for the greenhouse to be self-cooling:

$$\gamma = \frac{1}{\eta COP + 1} \qquad (7).$$

The calculation of $\eta$ depends on the type of solar collector used.

*4.1 Solar thermal collector without selective coating*

In this case the collector is considered a perfect blackbody, insulated from the surroundings such that convective or conductive losses are avoided. Nonetheless, there must occur radiation losses from the collector back to the surroundings as noted by several authors (e.g. Castañs [32] , De Vos [36], Müser [42]). For a simple black-body collector the maximum efficiency is accordingly [36]:

$$\eta = 1 - \frac{\left[T_h^4 - (1 - Cf)T_{sky}^4\right]}{CfT_{sun}^4} \qquad (8).$$

As well as including bidirectional radiation exchange with the sun, the expression includes radiation exchange with the sky at temperature $T_{sky}$ and it allows for the possible use of a concentrator, such as a mirror or lens, which reduces the area of the receiver by a factor $C$ for a given area over which sunlight is collected. The area $A$ of solar collection remains equal to $\gamma$ multiplied by the roof area of the greenhouse, with the aperture of the concentrating lens or mirror occupying $A$. The concentrator is assumed to be lossless.

Thus $\gamma$ can be determined from eqs. 3,4,7 and 8, given the input parameters $T_{c1}$, $T_{c2}$, $T_{sun}$, $T_{sky}$, $f$ and $C$. As regards $T_h$, this has to be optimized to maximize the product $\eta COP$, as $COP$ increases with $T_h$ while $\eta$ decreases. (See Appendix B for details of the optimization method). For $C$ =1 (no concentration) this results in $T_h$=365.5 K (92°C), $\eta$=0.56, $COP$ =3.07, and $\gamma$ = 0.367 (Table 2). Considering that the real value of $\gamma$ is likely to be substantially larger than this ideal minimum, this simple black body collector seems quite unpromising as it is likely to end up shading a large fraction (perhaps the entirety) of the greenhouse roof area. As shown in Fig. 3, $\gamma$ decreases with increasing $C$ until a theoretical minimum of $\gamma$=0.0571 occurs at $C$ =46300. The corresponding collector temperature is $T_h$=2479 K (2206°C).

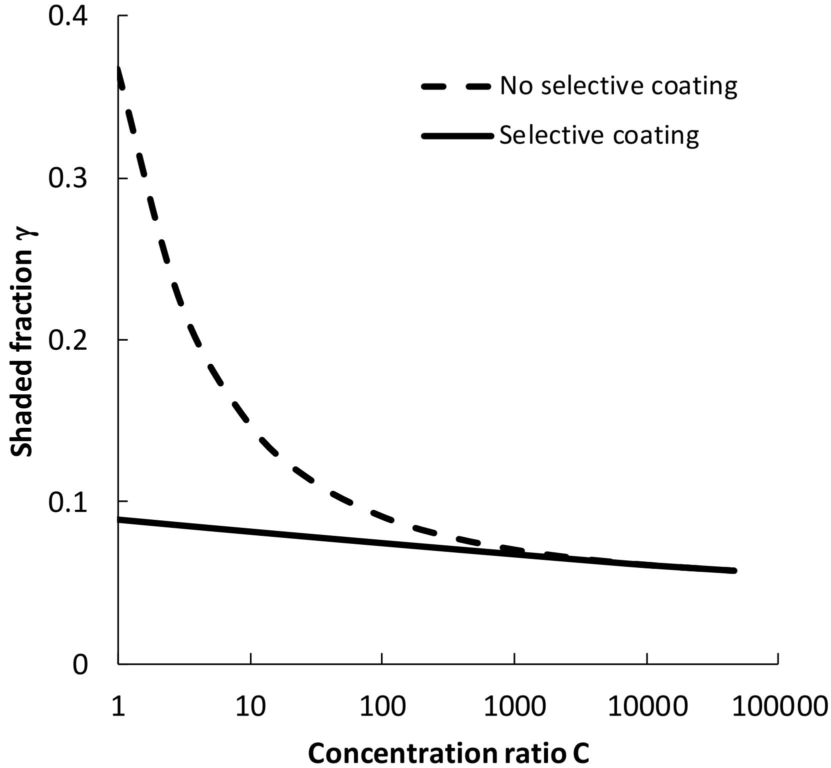


**Figure 3**: Minimum fraction $\gamma$ of greenhouse shaded by solar collector decreases with solar concentration ratio $C$, with more marked dependence in the case where no selective coating is used to decrease long-wave radiative losses. At maximum concentration ($C$=46300) the curves converge to $\gamma$=0.057 for cases with and without coating.

*4.2 Solar thermal collector with selective coating*

Selective optical coatings have long been used to improve the performance of solar thermal collectors. Following Castañs [32] the analysis for this case considers the solar radiation in two bands either side of a defined band gap $E_g$. For photons with energy $E<E_g$ there is no exchange of radiative energy between the sun (or sky) and the collector; while for photons with $E \geq E_g$ there is full exchange of black body radiation. Thus the net solar energy collected is given by the integration of Planck's law such that the collector efficiency for use in eq.(7) becomes:

$$\eta = \frac{1}{Cf\sigma T_{sun}^4} \frac{2\pi}{c^2 h^3} \int_{E_g}^{\infty} \left[ \frac{CfE^3}{\exp(E/kT_{sun}) - 1} + \frac{(1 - Cf)E^3}{\exp\left(E/kT_{sky}\right) - 1} - \frac{E^3}{\exp(E/kT_h) - 1} \right] dE \qquad (9).$$

Both $E_g$ and $T_h$ have to be optimized numerically to minimize $\gamma$ (see Appendix B) and the result at $C$=1 is: $E_g$=0.91 eV, $T_h$ = 849 K, $COP$ =12.5 and $\gamma$ =0.089 representing a considerable improvement on the previous value of $\gamma$=0.367 for the unselective collector. For the selective collector, increasing $C$ also improves performance eventually converging to the same minimum value of $\gamma$ as without the coating, since the optimized value of $E_g$ tends to zero with increasing $C$ – see Fig. 3 [32].

The collector with selective coating therefore seems more promising, even at $C$=1, but its implementation could be hampered by availability of materials to withstand such high temperature of $T_h$ = 849 K (576°C). In case this temperature has to be limited to lower values, Fig. 4 shows that $\gamma$ is not very sensitive to $T_h$ around the optimum, such that $\gamma$<0.1 is maintained at values down to $T_h$=615 K (342°C), while at $T_h$=473 K (200°C) $\gamma$=0.13. At 373K (100°C), however, $\gamma$ increases to 0.23.

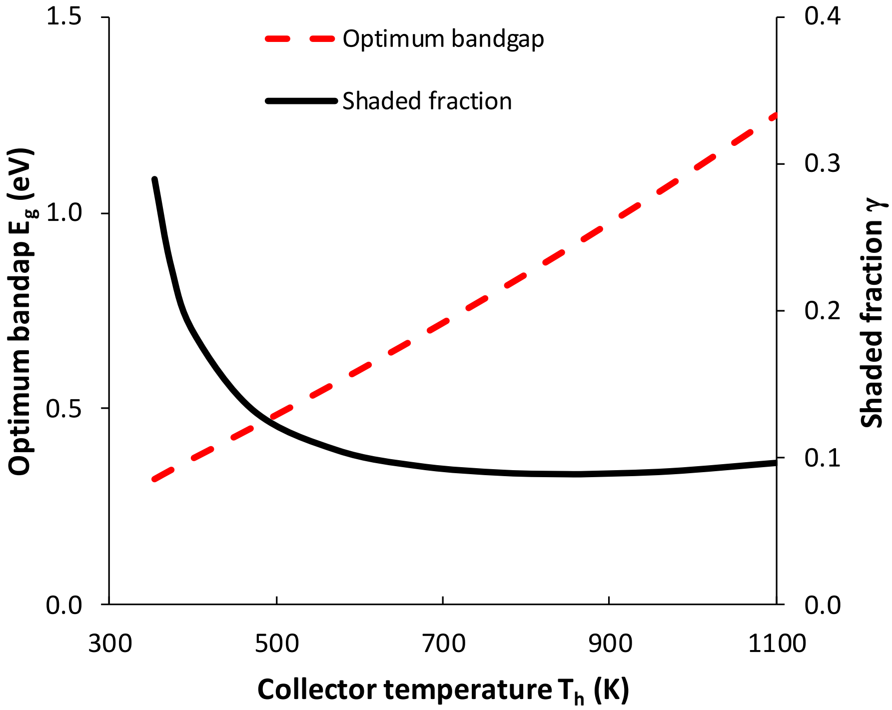


**Figure 4**: With a selective optical coating on the solar thermal collector ($C$=1), blocking outgoing longwave radiation below the bandgap $E_g$, a minimum value of $\gamma$=0.089 is obtained at $T_h$=849 K increasing to $\gamma$=0.23 at $T_h$=373 K.

## 5. Case of photovoltaic (PV) collector

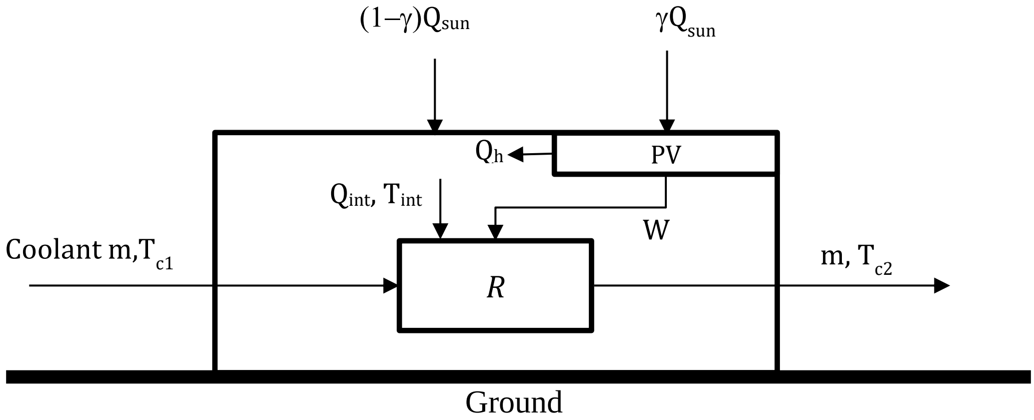


**Figure 5**: Case of the self-cooling greenhouse powered by a PV collector providing work at rate $W$ to a reversible refrigerator $R$ and rejecting heat $Q_h$ to the inside of the greenhouse.

For the analysis of the PV collector (Fig.5), it is assumed initially that the collector is housed inside the greenhouse, rejecting heat to the interior, and operating at the internal temperature $T_{int}$. Like the thermal collector, it receives solar energy at rate $\gamma Q_{sun}$. The efficiency of the PV collector $\eta$ is defined in the conventional way such that the work (i.e. electrical power) obtained from it is:

$$W = \eta\gamma Q_{sun} \tag{10}$$

We also define $\lambda$ such that the PV collector rejects a certain amount of heat to the interior of the greenhouse according to:

$$Q_h = \lambda\gamma Q_{sun} \tag{11}$$

This rejected heat adds to the heat to be removed by the refrigerator:

$$Q_{int} = Q_h + (1-\gamma)Q_{sun} \tag{12}$$

Corresponding to the earlier entropy and enthalpy balances of eqs (1) and (2), we obtain now:

$$\frac{Q_{int}}{T_{int}} = mc_p \ln\frac{T_{c2}}{T_{c1}} \tag{13}$$

and

$$W + Q_{int} = mc_p(T_{c2} - T_{c1}) \tag{14}$$

This time, with $COP$ defined in the normal way for a mechanically driven refrigerator as $Q_{int}/W$, we get the ideal value of:

$$COP = \frac{1}{\bar{T}/T_{int} - 1} \quad (15).$$

Expressing heat and work flows in terms of $Q_{sun}$ in the eqs. 10-12 above and rearranging for $\gamma$ gives:

$$\gamma = \frac{1}{\eta COP + 1 - \lambda} \quad (16).$$

The values of $\eta$ and $\lambda$ are obtained by applying the detailed balance procedure to the PV cell [25]. Like most PV devices available today, it is assumed to be of single-junction type. At any photon energy level above the bandgap $E_g$, we can calculate the net flow of photons converted into electrons based on the incoming flow of solar photons, from which we subtract the outgoing flow according to Planck's law modified by the bias voltage of the cell $V$. Once the net flow $dN$ is calculated for each small interval of wavelength $dE$, the total flow is integrated over the entire spectrum from $E_g$ to infinity:

$$N = \frac{2\pi A}{c^2 h^3} \int_{E_g}^{\infty} \left[ \frac{CfE^2}{\exp(E/kT_{sun}) - 1} - \frac{E^2}{\exp([E - qV]/kT_{cell}) - 1} \right] dE \quad (17),$$

where $c$ is the speed of light and $h$ is Planck's constant. The outgoing flux corresponds to radiative recombination which is an avoidable loss of solar cells. The current is then obtained as $I=Nq$ where $q$ is the elementary charge. Finally, the efficiency $\eta$ is obtained by dividing by the work output $W=IV$ by the total power of the black body spectrum falling on the receiver, as given by Stefan's law $ACf\sigma T_{sun}^4$.

The calculation of $\lambda$ is obtained from a similar detailed balance integration for the energy flux of from the net absorbed photons after radiative recombination:

$$Q_h = \frac{2\pi A}{c^2 h^3} \int_{E_g}^{\infty} \left[ \frac{CfE^3}{\exp(E/kT_{sun}) - 1} - \frac{E^3}{\exp([E - qV]/kT_{cell}) - 1} \right] dE \quad (18).$$

This allows the total energy absorbed by the solar cell to be calculated and then, by subtraction of the work term $W$, we obtain $Q_h$ and hence $\lambda = Q_h/ACf\sigma T_{sun}^4$. As such, $Q_h$ corresponds to thermalisation of carriers in the semiconductor from their initial excitation energy (corresponding to the energy level of incoming photons) to the energy level corresponding to the bias voltage $V$ at which electrical power is extracted. In the above, $A$ is the area of the solar cell which cancels out in the calculation of $\eta$ and $\lambda$.

Note that, strictly speaking, there is also a contribution to $N$ from the long wave radiation corresponding to $T_{sky}$ but this contribution is found to be negligible at values of $E_g$ of interest because long-wave radiation has much lower energy levels and is assumed to be simply reflected from the solar cell after passing through the semiconductor and bouncing off the back contact. Thus it does not contribute significantly to either $W$ or $Q_h$.

Minimisation of $\gamma$ requires optimization of both $E_g$ and $V$ (see Appendix B). Application of the above analysis to the baseline case (Table 1, at $C$=1 and $T_{c2}$=313 K) leads to optimal values of $E_g$=1.31 eV, V=0.973 V, resulting in $COP$ =19.6 and $\gamma$ =0.151, indicating that the minimum shaded fraction with a PV single-junction cell as the power source is 15%.

The optimal bandgap of about $E_g$=1.3 eV is the same as that already reported for an optimized solar cell at $C$=1 [27]. With increasing values of exit coolant temperature $T_{c2}$ , however, this value increases towards $E_g$=1.4 eV (see Fig. 6). This is because it is better to reduce the values of $\lambda$, and thus the additional heating load on the greenhouse, favouring higher bandgaps and operating voltages that minimize the thermalisation loss. The importance of this additional load increases with $T_{c2}$ which has the effect of decreasing $COP$. As these values of $COP$ are idealized, real values are likely to be considerably lower, which would favour higher $E_g$ even at moderate values of $T_{c2}$ . At a value of $T_{c2}$ = 353 K (80°C) $\gamma$ increases to $\gamma$ =0.307 with optimal $E_g$ =1.375 eV. This confirms that, although greater values of $T_{c2}$ result in an economy of coolant fluid and associated pumping power, they incur a penalty in the light entering the greenhouse for photosynthesis because the solar collector has to be larger.

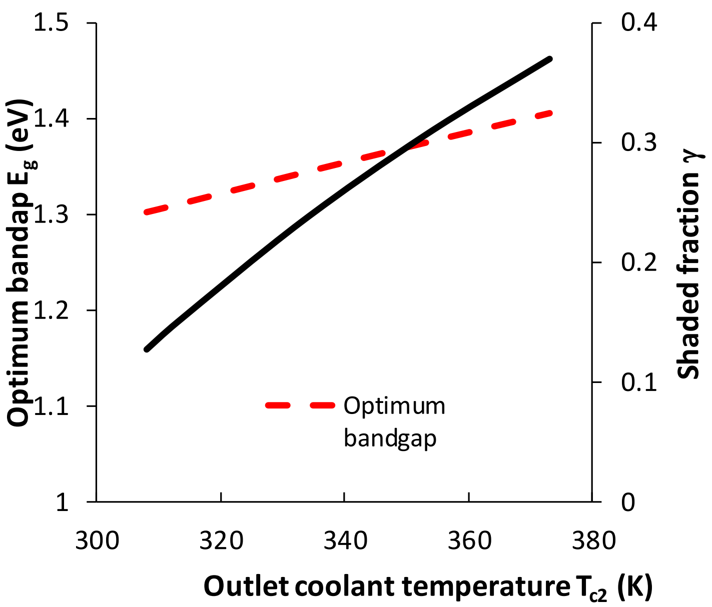


**Figure 6**: For the case of the PV self-cooling greenhouse, optimum bandgap $E_g$ and minimum shaded fraction $\gamma$ both increase with outlet coolant temperature $T_{c2}$.

Whereas the above results indicate an optimum bandgap of about $E_g$ =1.3 eV, this is not necessarily the preferred bandgap as it requires expensive semiconductors in the III-V family [43]. Silicon is by far the most common material for solar cell construction with $E_g$ =1.1 eV. Thus it is important to investigate the effect of $E_g$ on bandgap. Using eq.16 again, Fig.7 shows that the $\gamma$ is not very sensitive to $E_g$ remaining below 0.17 in the range $E_g$ =1–1.7 eV. Nonetheless, some organic PV materials have considerably higher bandgaps e.g. 6,6-phenyl C61-butyric acid methyl ester (PCBM) has $E_g$ =2.3 eV [19]. For this value, the minimum achievable shading is increased from $\gamma$=0.15 to 0.22 (Fig.7)

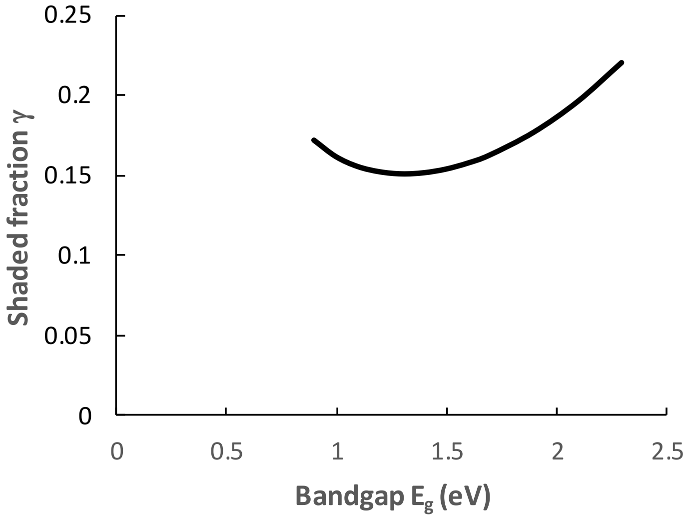


**Figure 7**: Effect of bandgap on minimum shaded fraction $\gamma$ around the optimum of $E_g$=1.3 eV for the solar PV collector.

The assumption in Fig. 5 and eq.(16), leading to the above results, is that the heat $Q_h$ rejected from the PV collector entirely enters the greenhouse. This seems a good assumption when the PV collector is internal to the greenhouse, as in the studies of Li, Yano, Cossu, Yasunori, Matsuoka, Nakamura, Matsumoto and Nakata [17] and Yano, Onoe and Nakata [14]. However, in other types of PV greenhouse the collectors are integrated with the cladding [19]; or they could even be mounted outside the cladding leaving an air gap. In the latter case, it would be reasonable to assume that $Q_h$ would not enter the greenhouse, and thus the term $\lambda$ would be eliminated from eq.(16) causing $\gamma$ to decrease from 0.151 to 0.143 with $T_h$ kept at 293 K. On the other hand, with the PV collector outside the greenhouse, its temperature $T_h$ must increase as it cannot be cooler than the surrounding air. Putting $T_h$ =308 K (35°C) increases $\gamma$ from 0.143 to 0.145. Since the value of $\gamma$ is not therefore very sensitive to these assumptions, it is concluded that $\gamma$ =0.15 is a reliable figure for the minimum shaded fraction in a single-junction PV self-cooled greenhouse under the baseline conditions of this study.

Whereas the above calculations for the PV case are all for unconcentrated sunlight ($C$=1) it is well known that the efficiency of solar cells can be improved under concentrated sunlight [29]. The resulting $\gamma$ has been calculated here for a range of concentrations for the cases of heat rejected both internally and externally (Fig.8). Both cases show a decrease in $\gamma$ by about 22% at the maximum possible value of C=46300 (ie. restoring the radiation to its intensity at the sun's surface) where, for the parameter values in Table 1 and heat rejected internally, $E_g$ =1.106 eV, $V$ =1.048 V, $COP$ =19.6 and $\gamma$ =0.116.

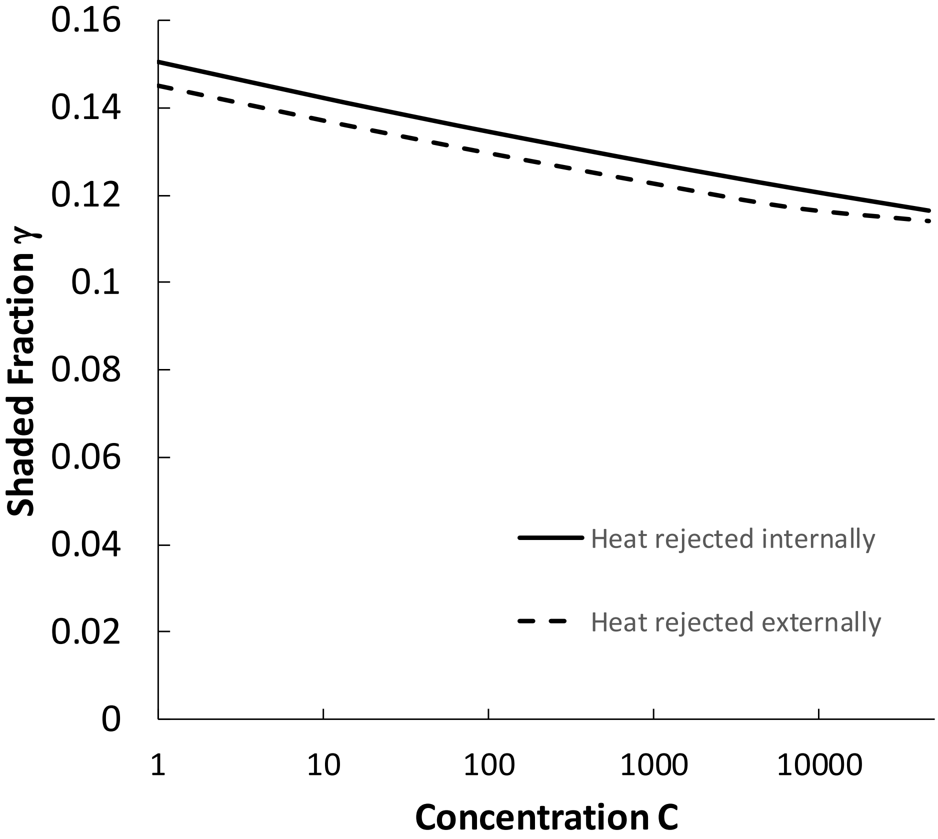


**Figure 8:** Effect of concentration ratio on the minimum shaded fraction $\gamma$ using a single-junction PV collector.

## 6. Ultimate limit: case of multiple solar collectors with spectrum splitting

De Vos [36] showed that an improvement to the single-temperature solar thermal collector working at optimized temperature is obtainable by splitting the incoming solar spectrum into many components of colour, with individual collectors each optimized in temperature according to the incoming photon energy level. It was also shown that the same analysis represents the limiting performance of a multi-junction PV cell for an infinite number of junctions. Although an infinite number of collectors or junctions cannot be practically realised, this case is included here to represent the ultimate performance for any solar-powered self-cooling greenhouse.

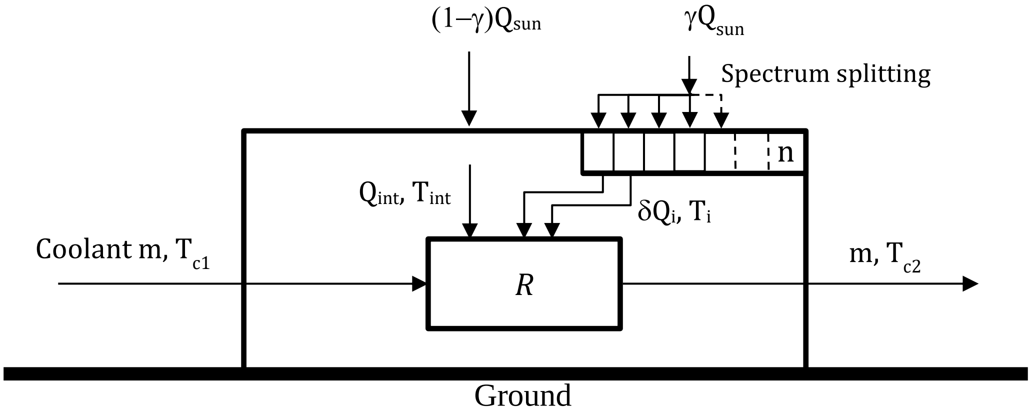


**Figure 9**: Idealised self-cooling greenhouses using multicolour solar energy conversion via a large number *n* of collectors each at optimised temperature, representing an ultimate limit for both thermal and PV cases.

We must now allow a series of heat sources to feed into the reversible thermally powered heat pump (Fig. 9) each one carrying its own heat and entropy flow. If there are in total *n* solar collectors, each receiving an amount of solar radiation $Q_i$ in the photon energy range $E_i$ to $E_i + \delta E$ according to Planck's law as:

$$\delta Q_i = \frac{2\pi A}{c^2 h^3} \int_{E_i}^{E_i+\delta E} \frac{E^3 dE}{\exp(E/kT_{sun}) - 1} \tag{19}$$

Each one also loses blackbody radiation at the rate:

$$\delta Q_{i\_loss} = \frac{2\pi A}{c^2 h^3} \int_{E_i}^{E_i+\delta E} \frac{E^3 dE}{\exp(E/kT_i) - 1} \tag{20}$$

Maximum concentration corresponding to $Cf$ =1 has been assumed for this ideal limiting case. The efficiency of solar collection is calculated by subtracting $\delta Q_{i\_loss}$ from $\delta Q_i$ and dividing by $\delta Q_i$. Thus each collector feeds heat at rate $\eta_i\,\delta Q_i$ into the reversible machine at temperature $T_i$. The entropy and enthalpy and balances for the reversible machine will now be respectively:

$$\sum_i^n \frac{\eta_i \delta Q_i}{T_i} + \frac{Q_{int}}{T_{int}} = mc_p \ln\frac{T_{c2}}{T_{c1}} \tag{21}$$

and

$$\sum_i^n \eta_i \delta Q_i + Q_{int} = mc_p(T_{c2} - T_{c1}) \tag{22}$$

Combining the above two equations gives:

$$\sum_i^n \delta Q_i \, \eta_i \left[1 - \frac{\bar{T}}{T_i}\right] = Q_{int}\left[\frac{\bar{T}}{T_{int}} - 1\right] \qquad (23).$$

The amount of heat removed $Q_{int}$ will be maximized when for each collector the product $\eta_i[1 - \bar{T}/T_i]$ is maximized by optimal choice of $T_i$. For the case of $\delta E \longrightarrow 0$ (infinitely many collectors) the collection efficiency becomes, as a function of the receiver temperature $T$,

$$\eta(T) = 1 - \frac{\exp(E/kT_{sun}) - 1}{\exp(E/kT) - 1} \qquad (24).$$

Defining $COP$ with respect to the total solar heat flow to the solar collector, that is as $COP = Q_{int}/\gamma Q_{sun}$, gives for the ideal case of infinitely many collectors:

$$COP = \frac{1}{\sigma {T_{sun}}^4 (\bar{T}/T_{int} - 1)} \frac{2\pi}{c^2 h^3} \int_0^\infty \frac{\eta(T)[1 - \bar{T}/T(E)]E^3 dE}{\exp(E/kT_{sun}) - 1} \qquad (25).$$

And from the overall heat balance according to this definition of $COP$:

$$\gamma = \frac{1}{1 + COP} \qquad (26).$$

The analogy with the infinitely-many junction PV collector arises when the temperature $T(E)$ in the integral of eq.(25) is replaced with an effective PV cell emission temperature $T = \bar{T}/(1 - qV/E)$, valid only under monochromatic illumination [44]. This is very similar to the procedure used by De Vos to arrive at the general result of 86.8% for the efficiency limit of both PV and solar thermal multicolour conversion [De Vos [36], Chapter 8]. By the same approach, we obtain here identical values of $COP$ and $\gamma$ for these two cases. The 'planet temperature, $T_p$' in the work of De Vos is replaced here by the logarithmic mean temperature, $\bar{T}$.

After the numerical calculation to optimise $T(E)$, maximising $COP$ and minimising $\gamma$, we obtain $COP$ =16.84 and $\gamma$ =0.0561, just a marginal improvement on the earlier value of $\gamma$ = 0.0571 for a single thermal collector at maximum concentration. Nonetheless, this is less than half the value of $\gamma$= 0.151 obtained in the single-junction PV case.

The shaded fraction $\gamma$ depends on the assumption about the internal temperature, so far taken as $T_{int}$ =293 K (20°C). However, different types of crops may require different temperatures for cultivation, so it is important to investigate the sensitivity of $\gamma$ to $T_{int}$ (Fig.10). With $T_{int}$ decreased to 283 K (10°C) the ultimate limit (i.e. multicolour collection) gives $\gamma$ increased substantially from 0.0561 to 0.093. Fig.10 also includes results for the other types of solar collection considered in this study, showing that γ generally increases significantly with decreasing $T_{int}$.

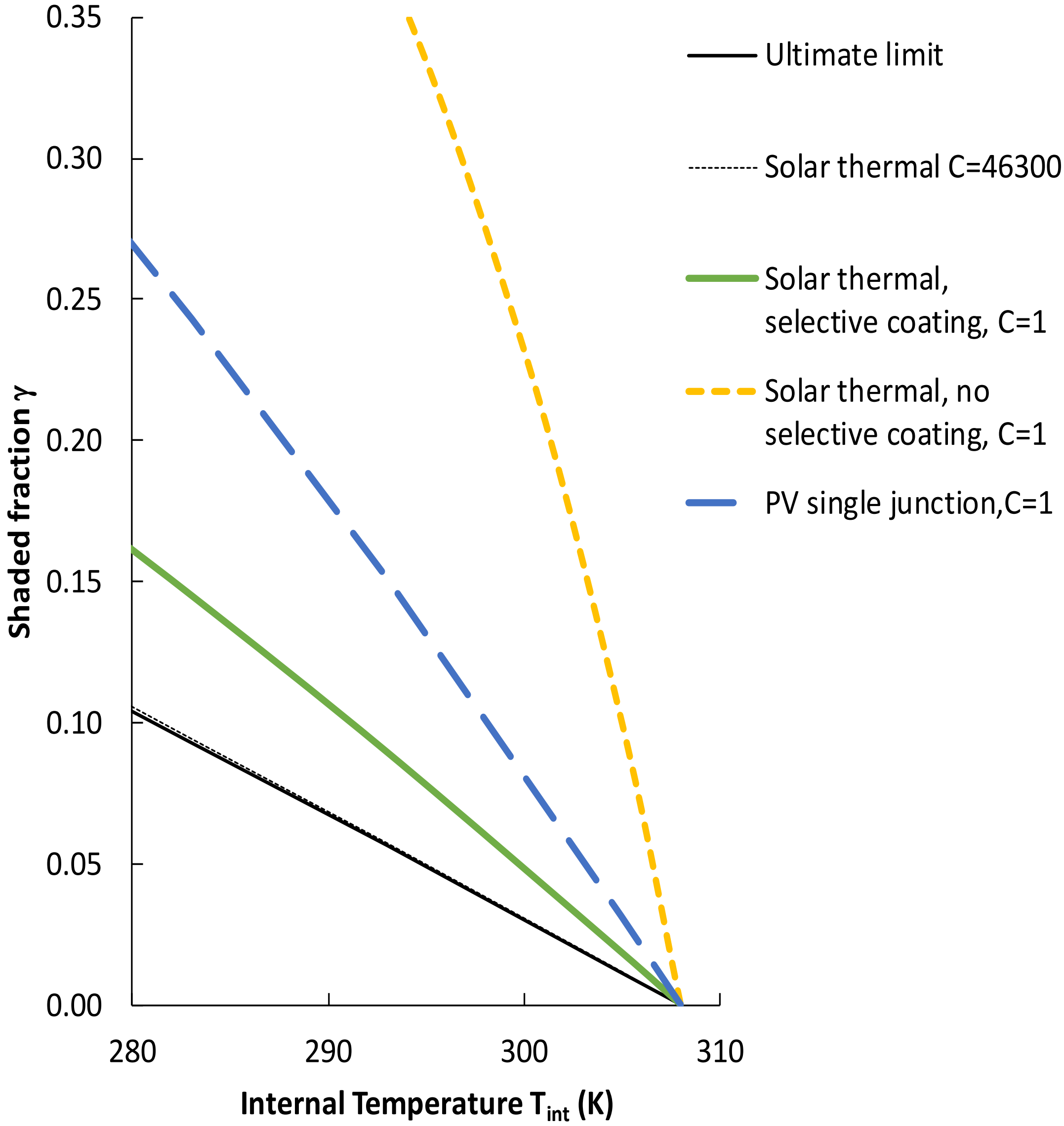


**Figure 10**: Shaded fraction γ increases as internal temperature decreases, by a different amount for each of the solar collector technologies considered.

**Table 2:** Summary of main results for the ideal minimum shaded fraction, $\gamma$, for different types of solar collector - based on parameters in Table 1.

| Type of solar collector | Modification | Solar concentration C | Collector temperature $T_h$ (°C) | Bandgap $E_g$ (eV) | Minimum $\gamma$ |
|---|---|---|---|---|---|
| Thermal | None | 1 | 92.5 | NA | 0.367 |
| | | 46300 | 2206 | NA | 0.057 |
| | Selective coating | 1 | 576 | 0.91 | 0.089 |
| | | 1 | 342 | 0.62 | 0.100 |
| | | 1 | 100 | 0.35 | 0.230 |
| | | 46300 | 2206 | 0 | 0.057 |
| PV (heat rejected into greenhouse) | NA | 1 | NA | 1.1 | 0.155 |
| | | 1 | NA | 1.3 | 0.151 |
| | | 1 | NA | 2.3 | 0.221 |
| | | 46300 | NA | 1.1 | 0.116 |
| Ultimate limit (thermal and PV) | NA | 46300 | NA | NA | 0.056 |

## 7. Discussion

Table 2 summarises the main results for the minimum shaded fraction $\gamma$ according to the different cases considered. Giving $\gamma$=0.15, the single-junction PV self-cooling greenhouse seems only marginally promising, because the real value of $\gamma$ achievable is likely to be considerably higher on account of losses in both the PV cell and the refrigeration machine it drives. Real PV cells have efficiencies rarely exceeding two-thirds the thermodynamic maximum; and real refrigeration machines have $COP$ of perhaps half the Carnot limit. These factors would increase $\gamma$ to at least 0.4 by eq. (16). As noted in the Introduction, such a high shaded fraction would likely reduce crop yield significantly.

On the other hand, improved future availability of multi-junction cells may make the PV self-cooling greenhouse viable. At $C$=1, a two-junction cell has ideal efficiency of 0.429, up from 0.31 for a single junction, reducing the ideal value of $\gamma$ from 0.15 to about 0.11 [36]. However, cost considerations in the proposed self-cooling greenhouse are likely to be crucial, as greenhouse crops have to compete with other modes of cultivation or imports from more temperate regions. Therefore a low-cost and efficient multi-junction PV device would be needed, unlike current commercial multi-junction devices which tend to be expensive.

As regards the solar-thermal self-cooling greenhouse, the simple blackbody collector is very unpromising without optical concentration ($C$=1) becoming more feasible as $C$ is increased above 10 (Fig.3). Sufficiently high concentration ratios cannot be achieved with simple static arrangements; instead tracking arrangements with at least one axis of motion would be required. Though this would introduce some mechanical complexity, it is interesting to note that Sonneveld, et al. [45] combined a static Fresnel lens with a tracking solar collector (achieving $C$=25) blocking out direct radiation and allowing only diffuse radiation to reach the crops. According to the current study, the minimum $\gamma$

possible at $C$=25 is $\gamma$=0.12 for a thermal collector without selective coating, decreasing to $\gamma$=0.08 with selective coating; and $\gamma$ =0.14 for a PV collector (Fig.3 and Fig.8 respectively). As an aside, we note that the collector studied by Sonneveld et al.[45] did not drive a refrigeration system, and was actually a hybrid photovoltaic-thermal collector. This hybrid case has not been considered here, and is an interesting case for future study.

According to the findings of this study, a solar thermal collector with selective optical coating appears promising, with $\gamma$=0.089 achievable without the need to concentrate the sunlight. Solar thermal collectors could be used, for example, to power desiccant cooling systems [46, 47]. Nonetheless, Fig. 4 shows that this can only be efficient if high temperatures (>250°C say) are used in the solar thermal collection. Stationery, high-temperature ultra-vacuum solar thermal collectors have recently become available with operating temperature approaching 200°C [48]. This approach would also require high-temperature materials for use in the rest of the refrigeration system. Lefers, et al. [49] suggested an arrangement whereby solar-powered membrane distillation is used for regeneration of a liquid desiccant, with the additional feature that transpired water is recovered for irrigation. High temperature ceramic or polymer membranes may be developed in future for use in such systems.

For the sake of generality, some simplifying assumptions have been made in this study, concerning in particular the sky temperature $T_{sky}$ which was set equal to the internal temperature $T_{int}$=293 K. To check the validity of this assumption, different values of sky temperature have also been tried in the case of the solar thermal collector (without selective coating). For this purpose, eq.(5) is modified to include an additional term representing exchange of radiation with the sky. The calculations, detailed in Appendix A, confirm that for concentrations up to $C$=1000, varying $T_{sky}$ by ± 10 K affects the resulting $\gamma$ by less than 5%.

This analysis is independent of the technological designs and materials and has been concerned only with a steady-state self-cooling greenhouse, neglecting any heat storage mechanisms. One contrasting example of a climate-controlled greenhouse for hot climates is offered by the *Watergy* project, which combined an internal heat exchanger with external reservoirs of water for heat storage allowing night-time cooling to be used [50-53]. This approach is particularly interesting for the Mediterranean climate, where substantial diurnal temperature swings occur. Extension of this analysis to consider supplementary night-time cooling is possible where good data on relevant ambient and perhaps sky temperature are available; however, the results will probably not be as general as they will depend on a larger number of input parameters.

Another topic for further study concerns the use of solar collectors that selectively allow certain spectral bands to pass into the greenhouse. An example of this proposed by Sonneveld, et al. [54] consisted of a greenhouse with a parabolic roof, providing a selective filter for photo-synthetically active radiation (PAR) while concentrating near-infrared (NIR) light for use in a solar collector of thermal, PV or hybrid type. The theory of blackbody absorbers could be extended to absorbers effective over different portions of the solar spectrum, resulting in expressions for efficiency generally similar to eq.(9) but with the integrals applied piecewise. Thus selective transmission could be designed to match the photosynthetic action spectrum of the plants, allowing $\gamma$ to be increased without sacrificing crop growth.

## 8. Conclusions

This paper has shown the theoretical feasibility of self-cooling greenhouses. The fraction of light intercepted to drive the refrigeration system can be as small as $\gamma$=0.056 at the ideal thermodynamic limit. Such a small shaded fraction would not affect significantly the yield of crops. Nevertheless, this theoretical limit requires very complex, multicolour solar energy conversion to be implemented with many collection stages each optimised for a different portion of the solar spectrum and with the incoming sunlight concentrated maximally ($C$=46300).

When more realistic concepts are considered, we obtain results ranging from $\gamma$ =0.089 for a thermal collector with a selective coating, $\gamma$ =0.151 for a single-junction PV cell, to $\gamma$ =0.367 for a thermal collector with no selective coating (in all cases without solar concentration, $C$=1). The results are sensitive to the target temperature of the greenhouse interior, $T_{int}$. Thus, the above value of $\gamma$ =0.089 obtained at $T_{int}$=20°C increases to $\gamma$=0.12 at $T_{int}$=15°C.

In general, realisation of the self-cooling greenhouse requires advances in solar energy conversion and refrigeration technologies beyond the current state of the art. It could require, for example, integrated optical concentrators together with multi-junction PV devices, or thermal refrigeration systems driven at high temperatures, requiring considerable R&D effort for cost-effective and efficient incorporation of such techniques into horticultural greenhouses. Once initial prototypes of self-cooling greenhouses become available, it will be interesting to compare their performance against the results given here. Such comparisons could be made with the help of an exergy analysis.

**Acknowledgements**
The authors acknowledge support under the European Commission (DG for Research & Innovation) 7th Framework Program SFERA-II project for access to EU research installations (Grant Agreement n. 312643)

## Appendix A: Effect of sky temperature

This appendix considers the sensitivity of the results to the assumption about sky temperature. Initially it was assumed $T_{sky}=T_{int}$ such that radiation exchange between the greenhouse interior and the sky was negligible. When modified to include radiation exchange with the sky, eq.(5) becomes:

$$Q_{int} = (1-\gamma)\left[Q_{sun} + A_g\sigma(T_{sky}^4 - T_{int}^4)\right]$$

where $A_g$ is the plan area of the greenhouse. The calculation for $\gamma$ now gives, in place of eq.(7),

$$\gamma = \frac{1+Z}{\eta COP + 1 + Z}$$

where

$$Z = \frac{1}{f}\left[\frac{T_{sky}^4 - T_{int}^4}{T_{sun}^4}\right]$$

Use of which gives the following results for γ at different sky temperatures and solar concentrations (solar thermal concentrator case without selective coating, $T_{int}$=293 K):

| | $T_{sky}$=$T_{int}$=293 K (baseline) | $T_{sky}$=283 K | $T_{sky}$=303 K |
|---|---|---|---|
| $C$=1 | 0.367 | 0.376 | 0.360 |
| $C$=30 | 0.112 | 0.109 | 0.116 |
| $C$=100 | 0.0907 | 0.0874 | 0.0943 |
| $C$=300 | 0.0787 | 0.0758 | 0.0819 |
| $C$=1000 | 0.0701 | 0.0675 | 0.0730 |

The results show a variation in γ of <5% with ± 10 K change in $T_{sky}$.

## Appendix B: Optimisation methods

This appendix explains numerical details used in the various optimisation calculations to minimise the value of γ. The Generalised Reduced Gradient (GRG) method from the Solver toolbox of Excel® was used. For the case of the solar thermal without coating (section 4.1) this method was used to optimise $T_h$. For the case of the solar thermal with selective coating (section 4.2) the GRG method was used to simultaneously optimise $E_g$ and $T_h$. To calculate the integral in eq.(9), the range of $E$ was divided into 100 steps between $E_g$ and $E$=3 eV, then above 3 eV it was divided into 0.25 eV increments up to 8 eV where the integral was truncated. Integration was done using the trapezium rule. For the case of the PV collector (section 5) the GRG method was used to optimise variables $E_g$ and $V/E_g$ with eqs.(17) and (18) integrated similarly to above. For the PV collector with multiple solar collectors (section 6) the values of $T$ were optimised (again using the GRG method) at each discrete value of $E$ used in the numerical integration of eq.(25). The convergence criterion for the GRG method was kept ≤0.0001 throughout. Results were verified against those available in reference [36] where applicable.

## References


1. WMO, Statement on the State of the Global Climate in 2017. In 2018.
2. PRB *World Population Data Sheet*; 2017.
3. Kumar, K.; Tiwari, K.; Jha, M. K., Design and technology for greenhouse cooling in tropical and subtropical regions: A review. *Energy and Buildings* **2009,** *41*, (12), 1269-1275.
4. Sethi, V. P.; Sharma, S. K., Survey of cooling technologies for worldwide agricultural greenhouse applications. *Solar Energy* **2007,** *81*, (12), 1447-1459.
5. Watt, J., *Evaporative air conditioning handbook*. Springer Science & Business Media: 2012.
6. Yang, S.-H.; Rhee, J. Y., Utilization and performance evaluation of a surplus air heat pump system for greenhouse cooling and heating. *Applied Energy* **2013,** *105*, 244-251.
7. Campen, J.; De Zwart, F.; Mohammed, A.; Ali, A.; Mohammed, D., Climatisation of a closed greenhouse in the Middle East. In *GreenSys 2017, International Symposium on New Technologies for Environment Control, Energy-saving and Crop Production in Greenhouse and Plant Factory*, Beijing, 2017.
8. Puglisi, G.; Vox, G.; Schettini, E.; Morosinotto, G.; Campiotti, C., Climate Control Inside Greenhouses by a Means of a Solar Cooling System. In *GreenSys 2017, International Symposium on New Technologies for Environment Control, Energy-saving and Crop Production in Greenhouse and Plant Factory*, Beijing, 2017.
9. Lychnos, G.; Davies, P. A., Modelling and experimental verification of a solar-powered liquid desiccant cooling system for greenhouse food production in hot climates. *Energy* **2012,** *40*, (1), 116-130.
10. Ng, P. K.; Mithraratne, N., Lifetime performance of semi-transparent building-integrated photovoltaic (BIPV) glazing systems in the tropics. *Renewable and Sustainable Energy Reviews* **2014,** *31*, 736-745.
11. Cucchiella, F.; D'Adamo, I.; Koh, S. L., Environmental and economic analysis of building integrated photovoltaic systems in Italian regions. *Journal of Cleaner Production* **2015,** *98*, 241-252.
12. Kadowaki, M.; Yano, A.; Ishizu, F.; Tanaka, T.; Noda, S., Effects of greenhouse photovoltaic array shading on Welsh onion growth. *Biosystems Engineering* **2012,** *111*, (3), 290-297.
13. Pérez-Alonso, J.; Pérez-García, M.; Pasamontes-Romera, M.; Callejón-Ferre, A. J., Performance analysis and neural modelling of a greenhouse integrated photovoltaic system. *Renewable and Sustainable Energy Reviews* **2012,** *16*, (7), 4675-4685.
14. Yano, A.; Onoe, M.; Nakata, J., Prototype semi-transparent photovoltaic modules for greenhouse roof applications. *Biosystems Engineering* **2014,** *122*, 62-73.
15. Hassanien, R. H. E.; Li, M.; Yin, F., The integration of semi-transparent photovoltaics on greenhouse roof for energy and plant production. *Renewable Energy* **2018,** *121*, 377-388.
16. Castellano, S.; Santamaria, P.; Serio, F. J. J. o. A. E., Solar radiation distribution inside a monospan greenhouse with the roof entirely covered by photovoltaic panels. **2016,** *47*, (1), 1-6.

17. Li, Z.; Yano, A.; Cossu, M.; Yasunori, K.; Matsuoka, T.; Nakamura, H.; Matsumoto, T.; Nakata, J., Prototype Greenhouse Blind-type Shading System Using a Semi-transparent Photovoltaic Module. In *GreenSys 2017, International Symposium on New Technologies for Environment Control, Energy-saving and Crop Production in Greenhouse and Plant Factory*, Beijing, 2017.
18. Li, Z.; Yano, A.; Cossu, M.; Yoshioka, H.; Kita, I.; Ibaraki, Y., Electrical Energy Producing Greenhouse Shading System with a Semi-Transparent Photovoltaic Blind Based on Micro-Spherical Solar Cells. *Energies* **2018,** *11*, (7), 1681.
19. Emmott, C. J.; Röhr, J. A.; Campoy-Quiles, M.; Kirchartz, T.; Urbina, A.; Ekins-Daukes, N. J.; Nelson, J., Organic photovoltaic greenhouses: a unique application for semi-transparent PV? *Energy & environmental science* **2015,** *8*, (4), 1317-1328.
20. Allardyce, C. S.; Fankhauser, C.; Zakeeruddin, S. M.; Grätzel, M.; Dyson, P. J., The influence of greenhouse-integrated photovoltaics on crop production. *Solar Energy* **2017,** *155*, (Supplement C), 517-522.
21. Dupraz, C.; Marrou, H.; Talbot, G.; Dufour, L.; Nogier, A.; Ferard, Y., Combining solar photovoltaic panels and food crops for optimising land use: Towards new agrivoltaic schemes. *Renewable Energy* **2011,** *36*, (10), 2725-2732.
22. Marcelis, L. F. M.; Broekhuijsen, A. G. M.; Meinen, E.; Nijs, E. M. F. M.; Raaphorst, M. G. M. In *Quantification of the growth response to light quantity of greenhouse grown crops*, 2006; International Society for Horticultural Science (ISHS), Leuven, Belgium: 2006; pp 97-104.
23. Thomas, M. D., Effect of ecological factors on photosynthesis. *Annual Review of Plant physiology* **1955,** *6*, (1), 135-156.
24. Blackman, F. F., Optima and Limiting Factors. *Annals of Botany* **1905,** *19*, (74), 281-295.
25. Shockley, W.; Queisser, H. J., Detailed balance limit of efficiency of p‐n junction solar cells. *Journal of applied physics* **1961,** *32*, (3), 510-519.
26. Trivich, D.; Flinn, P., Maximum efficiency of solar energy conversion by quantum processes. *Solar Energy Research* **1955**, 143.
27. Araújo, G. L.; Martí, A., Absolute limiting efficiencies for photovoltaic energy conversion. *Solar Energy Materials and Solar Cells* **1994,** *33*, (2), 213-240.
28. Landsberg, P.; Mallinson, J. In *Thermodynamic constraints, effective temperatures and solar cells*, International Conference on Solar Electricity, 1976; 1976; pp 27-42.
29. Henry, C. H., Limiting efficiencies of ideal single and multiple energy gap terrestrial solar cells. *Journal of applied physics* **1980,** *51*, (8), 4494-4500.
30. Marti, A.; Araújo, G. L., Limiting efficiencies for photovoltaic energy conversion in multigap systems. *Solar Energy Materials and Solar Cells* **1996,** *43*, (2), 203-222.
31. Markvart, T.; Bauer, G. H., What is the useful energy of a photon? *Applied Physics Letters* **2012,** *101*, (19), 193901.
32. Castañs, M., Bases fisicas del aprovechamiento de la energia solar. *Revista Geofisica* **1976,** *35*, 227.
33. De Vos, A., Efficiency of some heat engines at maximum‐power conditions. *American Journal of Physics* **1985,** *53*, (6), 570-573.

34. Jones, A.; Underwood, C., A thermal model for photovoltaic systems. *Solar energy* **2001,** *70*, (4), 349-359.
35. Adelard, L.; Pignolet-Tardan, F.; Mara, T.; Lauret, P.; Garde, F.; Boyer, H., Sky temperature modelisation and applications in building simulation. *Renewable Energy* **1998,** *15*, (1-4), 418-430.
36. De Vos, A., *Thermodynamics of solar energy conversion*. John Wiley & Sons: 2008.
37. Sørensen, B., *Renewable energy conversion, transmission, and storage*. Academic press: 2007.
38. Al-Subhi, A. M., Temporal and spatial distribution of the remotely sensed sea surface temperature in the northern Red Sea. *Journal of KAU-MArine Sciences* **2008,** *19*, (1).
39. Elliott, M. *Thermal standards for cooling water from new build nuclear power stations*; British Energy Estuarine and Marine Studies: 2011.
40. von Zabeltitz, C., Crop Growth Requirements and Climate Control. In *Integrated Greenhouse Systems for Mild Climates: Climate Conditions, Design, Construction, Maintenance, Climate Control*, von Zabeltitz, C., Ed. Springer Berlin Heidelberg: Berlin, Heidelberg, 2011; pp 29-43.
41. Rubin, M. H., Optimal configuration of a class of irreversible heat engines. I. *Physical Review A* **1979,** *19*, (3), 1272.
42. Müser, H. A., Thermodynamische behandlung von elektronenprozessen in halbleiter-randschichten. *Zeitschrift für Physik A Hadrons and Nuclei* **1957,** *148*, (3), 380-390.
43. Nelson, J., *The physics of solar cells*. World Scientific Publishing Co Inc: 2003.
44. Davies, P.; Luque, A., Solar thermophotovoltaics: brief review and a new look. *Solar energy materials and solar cells* **1994,** *33*, (1), 11-22.
45. Sonneveld, P. J.; Swinkels, G. L. A. M.; Tuijl, B. A. J. v.; Janssen, H. J. J.; Campen, J.; Bot, G. P. A., Performance of a concentrated photovoltaic energy system with static linear Fresnel lenses. *Solar Energy* **2011,** *85*, (3), 432-442.
46. Davies, P. A., A solar cooling system for greenhouse food production in hot climates. *Solar Energy* **2005,** *79*, (6), 661-668.
47. Banik, P.; Ganguly, A., Performance and economic analysis of a floricultural greenhouse with distributed fan-pad evaporative cooling coupled with solar desiccation. *Solar Energy* **2017,** *147*, 439-447.
48. Calise, F.; d'Accadia, M. D.; Vicidomini, M.; Scarpellino, M., Design and simulation of a prototype of a small-scale solar CHP system based on evacuated flat-plate solar collectors and Organic Rankine Cycle. *Energy Conversion and Management* **2015,** *90*, 347-363.
49. Lefers, R.; Bettahalli, N. M. S.; Nunes, S. P.; Fedoroff, N.; Davies, P. A.; Leiknes, T., Liquid desiccant dehumidification and regeneration process to meet cooling and freshwater needs of desert greenhouses. *Desalination and Water Treatment* **2016,** *57*, (48-49), 23430-23442.
50. Zaragoza, G.; Buchholz, M., Closed greenhouses for semi-arid climates: Critical discussion following the results of the Watergy prototype. In *Acta Horticulturae*, 2008; Vol. 797, pp 37-42.
51. Buchholz, M.; Jochum, P.; Zaragoza, G., Concept for water, heat and food supply from a closed greenhouse -the watergy project. In *Acta Horticulturae*, 2005; Vol. 691, pp 509-516.

52. Buchholz, M.; Buchholz, R.; Jochum, P.; Zaragoza, G.; Pérez-Parra, J., Temperature and humidity control in the Watergy greenhouse. In 719 ed.; Acta Horticulturae: 2006; pp 401-408.
53. Zaragoza, G.; Buchholz, M.; Jochum, P.; Pérez-Parra, J., Watergy project: Towards a rational use of water in greenhouse agriculture and sustainable architecture. *Desalination* **2007,** *211*, (1), 296-303.
54. Sonneveld, P. J.; Swinkels, G. L. A. M.; Bot, G. P. A.; Flamand, G., Feasibility study for combining cooling and high grade energy production in a solar greenhouse. *Biosystems Engineering* **2010,** *105*, (1), 51-58.